Nonlinear Analysis: Real World Applications 14 (2013) 455–464

Contents lists available at SciVerse ScienceDirect

Nonlinear Analysis: Real World Applications

journal homepage: www.elsevier.com/locate/nonrwa

Unsteady convective boundary layer flow of a viscous fluid at a vertical surface with variable fluid properties

K. Vajravelu [a,*], K.V. Prasad [b], Chiu-On Ng [c]

[a] Department of Mathematics, University of Central Florida, Orlando, FL 32816, USA

[b] Department of Mathematics, Bangalore University, Bangalore 560001, India

[c] Department of Mechanical Engineering, The University of Hong Kong, Hong Kong, China

ARTICLE INFO

Article history:
Received 1 July 2011
Accepted 6 July 2012

Keywords:
Unsteady boundary layers
Variable thermal conductivity
Thermal radiation
Heat transfer
Mixed convection

ABSTRACT

In this paper we present numerical solutions to the unsteady convective boundary layer flow of a viscous fluid at a vertical stretching surface with variable transport properties and thermal radiation. Both assisting and opposing buoyant flow situations are considered. Using a similarity transformation, the governing time-dependent partial differential equations are first transformed into coupled, non-linear ordinary differential equations with variable coefficients. Numerical solutions to these equations subject to appropriate boundary conditions are obtained by a second order finite difference scheme known as the Keller-Box method. The numerical results thus obtained are analyzed for the effects of the pertinent parameters namely, the unsteady parameter, the free convection parameter, the suction/injection parameter, the Prandtl number, the thermal conductivity parameter and the thermal radiation parameter on the flow and heat transfer characteristics. It is worth mentioning that the momentum and thermal boundary layer thicknesses decrease with an increase in the unsteady parameter.

1. Introduction

The study of two-dimensional boundary layer flow and heat transfer induced by continuous stretching and heated surfaces has acquired momentum due to its various applications in engineering/industrial disciplines. These applications include extrusion processes, wire and fiber coating, polymer processing, food-stuff processing, design of heat exchangers, and chemical processing equipment. The concept of continuous stretching will bring in a unidirectional orientation to the extrudate; consequently the quality of the final product considerably depends on the flow and heat transfer mechanism. To that end, the analysis of momentum and thermal transports within the fluid on a continuously stretching surface is important for gaining some fundamental understanding of such processes. Sakiadis [1] was the first amongst others to initiate such a problem by considering the boundary layer fluid flow over a continuous solid surface moving with constant velocity. The thermal behavior of the problem was studied by Erickson et al. [2], and experimentally verified by Tsou et al. [3]. Crane [4] extended the work of Sakiadis [1] to the flow caused by an elastic sheet moving in its own plane with a velocity varying linearly with the distance from a fixed point. Also, heat and mass transfer aspects with Newtonian/non-Newtonian fluids are studied by several authors [5–11] under different physical situations.

All the above studies deal with fluid flows and heat transfer in the absence of a buoyancy force. In many practical situations the material moves in a quiescent fluid due to the fluid flow induced by the motion of the solid material and/or by the thermal buoyancy. Therefore the resulting flow and the thermal field are determined by these two mechanisms,

* Corresponding author.
E-mail addresses: kuppalapalle.vajravelu@ucf.edu, vajravel@mail.ucf.edu (K. Vajravelu).

1468-1218/$ – see front matter © 2012 Elsevier Ltd. All rights reserved.
doi:10.1016/j.nonrwa.2012.07.008

Nomenclature

a, b, c, B_2	Constants
A	Unsteady parameter
C_f	Skin friction
C_p	Specific heat at constant pressure
f	Dimensionless stream function
f_w	Surface mass transfer parameter
g	Acceleration due to gravity
$k(T)$	Thermal conductivity
k_w	Thermal conductivity at the sheet
k_∞	Thermal conductivity far away from the sheet
M	Kummer's function
Nu_x	Nusselt number
Nr	Thermal radiation parameter
Pr	Prandtl number
q_w	Local heat flux at the sheet
q_r	Radiative heat flux
T	Fluid temperature
T_w	Given temperature at the sheet
T_∞	Constant temperature of the fluid far away from the sheet
t	Time
x	Horizontal distance
y	Vertical distance
u	Velocity in x direction
U_w	Velocity of the stretching surface
v_w	Suction/blowing velocity
v	velocity in y direction

Greek symbols

α_∞	Thermal diffusivity
ΔT	Sheet temperature
ε	Small parameter
η	Similarity variable
ν	Kinematic viscosity
β	Thermal expansion coefficient
μ	Dynamic viscosity
ψ	Stream function
ρ	Density
σ^*	Stephan–Boltzmann constant
k^*	Mean absorption coefficient
τ_{xy}	Shear stress
θ	Dimensionless temperature variable
λ	Free convection or buoyancy parameter

i.e., surface motion and thermal buoyancy. It is well known that the buoyancy force stemming from the heating or cooling of the continuous stretching sheet alters the flow and the thermal fields and thereby the heat transfer characteristics of the manufacturing processes. However, the buoyancy force effects were not considered in the aforementioned studies. Effects of thermal buoyancy on the flow and heat transfer over a stretching sheet were reported by several investigators (see for details [12–20]). Combined free and forced convection heat transfer at a stretching sheet with variable temperature and linear velocity was investigated by Vajravelu [12]. Similar analyses were performed numerically by Chen and Strobel [13], and Moutsoglou and Chen [14] for Newtonian fluids under different physical situations. An analysis has been carried out by Chen [15] for laminar mixed convection in a boundary layer adjacent to a vertical continuously stretching sheet. Hamad et al. [19] discussed the similarity reduction for the free convection flow of a nanofluid past a semi-infinite vertical flat plate in the presence of transverse magnetic field. Recently, Sarkar et al. [20] investigated the buoyancy driven mixed convective flow and heat transfer characteristics of water-based nanofluid past a circular cylinder.

All the above studies deal with only the steady flow. However, in reality the flow and heat transfer problems are unsteady in nature, due to a sudden stretching of the flat sheet or due to the change in the temperature of the sheet. When the

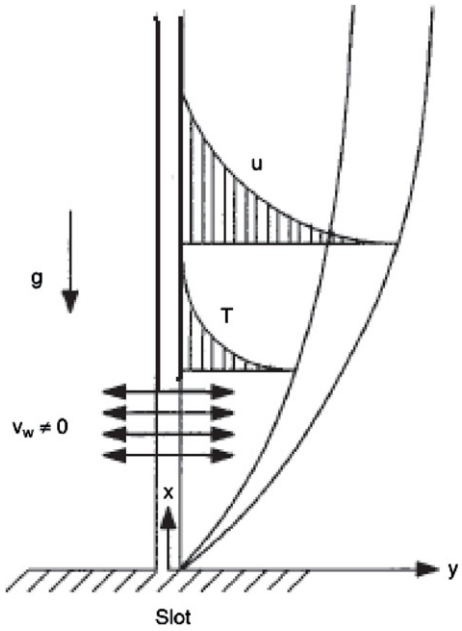

Fig. 1. Physical model and coordinate system.

surface is impulsively stretched with certain velocity, the inviscid flow is developed instantaneously. However, the flow in the viscous layer near the sheet is developed slowly, and it becomes a fully developed (steady) flow after a certain instant of time. Elbashbeshy and Bazid [21] presented a similarity solution for the boundary layer equations, which describe the unsteady flow and heat transfer over a stretching sheet and were extended by Abd El-Aziz [22] for some physical realistic phenomena. Mukhopadhyay [23] analyzed the effect of variable fluid properties on the unsteady fluid flow and heat transfer over a stretching sheet in the presence of suction. Ishak et al. [24] investigated the unsteady two-dimensional mixed convection boundary layer flow and heat transfer at a vertical stretching sheet. Kousar and Liao [25] presented an analytical solution to the unsteady non-similarity boundary-layer flows caused by an impulsively stretching flat sheet. Also, Rohini et al. [26] studied numerically the unsteady mixed convection flow near the stagnation point on a vertical permeable surface embedded in a fluid-saturated porous medium with suction and temperature slip effect. In all these studies, the thermo-physical properties of the fluids were assumed to be constant. However, it is well known that these properties may change with temperature, especially the thermal conductivity. Available literature on variable thermal conductivity [27–31] shows that the combined effects of variable thermal conductivity and thermal buoyancy has not been investigated for unsteady fluid flow and heat transfer over a porous stretching sheet.

Motivated by these applications, the present study explores the effects of variable thermal conductivity, thermal radiation and the thermal buoyancy on the unsteady fluid flow and heat transfer at a vertical porous stretching sheet. In contrast to the work of Ishak et al. [24], the effects of variable thermal conductivity and thermal radiation are included here; as this is true in some polymer solutions: Thermal radiation plays a significant role in controlling the heat transfer in the polymer processing industry. The quality of the final product depends to a great extent on the heat controlling factors, and the knowledge of radiative heat transfer in the system can perhaps lead to a desired product with sought qualities. The governing coupled, non-linear partial differential equations of the flow and heat transfer problem are transformed into non-linear, coupled ordinary differential equations with variable coefficients by using a similarity transformation. These coupled non-linear ordinary differential equations with variable coefficients subject to the appropriate boundary conditions are solved numerically by the Keller-box method for several sets of values of the physical parameters.

2. Mathematical formulation

Consider the unsteady laminar two-dimensional boundary layer flow of a viscous incompressible fluid past a semi-infinite porous stretching sheet coinciding with the plane $y = 0$ (Fig. 1). The Cartesian coordinate system has its origin located at the leading edge of the sheet with the positive x-axis extending along the sheet in the upwards direction, while the y-axis is measured normal to the surface of the sheet and is positive in the direction from the sheet to the fluid. We assume that for time $t < 0$ the fluid and heat flows are steady. The unsteady fluid and heat flows start at $t = 0$, the sheet is being stretched with the velocity $U_w(x, t)$ along the x-axis, keeping the origin fixed. The temperature of the sheet $T_w(x, t)$ is assumed to be a linear function of x. The thermo-physical properties of the sheet and the ambient fluid are assumed to be constant except density variations and the thermal conductivity which are assumed to vary linearly with temperature. Under

these assumptions (with the Boussinesq and boundary layer approximations), the governing equations for the convective flow and heat transfer of the viscous fluid (see Refs. [23,27,32–34]) are:

$$\frac{\partial u}{\partial x}+\frac{\partial v}{\partial y}=0, \tag{2.1}$$

$$\frac{\partial u}{\partial t}+u\frac{\partial u}{\partial x}+v\frac{\partial u}{\partial y}=\nu\frac{\partial^2 u}{\partial y^2}\pm g\beta\left(T-T_\infty\right), \tag{2.2}$$

$$\rho C_p\left(\frac{\partial T}{\partial t}+u\frac{\partial T}{\partial x}+v\frac{\partial T}{\partial y}\right)=\frac{\partial}{\partial y}\left(K(T)\frac{\partial T}{\partial y}\right)-\frac{\partial q_r}{\partial y}, \tag{2.3}$$

subjected to the boundary conditions

$$\begin{aligned} &u=U_w \qquad v=v_w(t) \qquad T=T_w \quad \text{at } y=0,\\ &u\to 0 \qquad T\to T_\infty \quad \text{as } y\to\infty, \end{aligned} \tag{2.4}$$

where u and v are the velocity components in the x and y directions, respectively, ν is the kinematic viscosity, g is the acceleration due to gravity, β is the coefficient of thermal expansion, T is the fluid temperature, T_∞ is the ambient temperature, ρ is the density, C_p is the specific heat at constant pressure, $K(T)$ is the variable thermal conductivity, $v_w(t)=v_0/\sqrt{1-ct}$ is the suction/injection velocity and q_r is the radiative heat flux. The last term in Eq. (2.2) is due to the buoyancy force. The "+" and "−" signs refer to the buoyancy assisting and buoyancy opposing flow situations, respectively. Here in this paper the thermal conductivity is assumed to vary linearly with temperature [27] as:

$$K(T)=K_\infty\left(1+\frac{\varepsilon}{\Delta T}\left(T-T_\infty\right)\right). \tag{2.5}$$

Here, $\Delta T=\left(T_w-T_\infty\right)$, T_w is the surface temperature, ε is a small parameter known as the variable thermal conductivity parameter, and K_∞ is the thermal conductivity of the fluid far away from the sheet. The radiative heat flux can be expressed (Roseland approximation by Brewster [35]) as

$$q_r=-\frac{4\sigma^*}{3k^*}\frac{\partial T^4}{\partial y}. \tag{2.6}$$

Here, σ^* and k^* are respectively, the Stephan–Boltzmann constant and the mean absorption coefficient. We assume that the temperature difference within the flow is such that the term T^4 can be expressed as a linear function of temperature. Hence, expanding T^4 in a Taylor series about T_∞ and neglecting higher-order terms, we obtain

$$T^4\approx 4T_\infty^3T-T_\infty^4. \tag{2.7}$$

Following Ishak et al. [24], the stretching velocity is assumed as $U_w(x,t)=ax/\left(1-ct\right)$ where a and c are constants (with $a\geq 0$ and $c\geq 0$ where $ct<1$), and both have dimension t^{-1}, we have a as the initial stretching rate $a/\left(1-ct\right)$ and it is increasing with time. In the context of polymer extrusion, the material properties, in particular the elasticity of the extruded sheet may vary with time even though the sheet is being stretched by a constant force. With unsteady stretching, however, a^{-1} becomes the representative time scale of the resulting unsteady boundary layer problem. We assume the surface temperature $T_w(x,t)$ of the stretching sheet to vary with the distance x and an inverse square law for its decrease with time in the following form:

$$T_w(x,t)=T_\infty+\frac{bx}{\left(1-ct\right)^2}. \tag{2.8}$$

Here b is a constant and has a dimension temperature/length, with $b>0$ and $b<0$ corresponding to the assisting and opposing flows, respectively, and $b=0$ is for the forced convection limit (absence of buoyancy force). These particular forms of $U_w(x,t)$ and $T_w(x,t)$ have been chosen in order to obtain a new similarity transformation, which transforms the governing partial differential equations (2.1)–(2.3) into a set of coupled ordinary differential equations with variable coefficients. Defining the following dimensionless functions f and θ, and the similarity variable η as

$$\eta=\left(\frac{a}{\nu\left(1-ct\right)}\right)^{\frac{1}{2}}y, \qquad \psi=\left(\frac{\nu a}{\left(1-ct\right)}\right)^{\frac{1}{2}}xf\left(\eta\right), \qquad \theta\left(\eta\right)=\frac{\left(T-T_\infty\right)}{\left(T_w-T_\infty\right)}, \tag{2.9}$$

where, $\psi\left(x,y,t\right)$ is a stream function defined as $(u,v)=\left(\partial\psi/\partial y,-\partial\psi/\partial x\right)$ which identically satisfies the mass conservation Eq. (2.1). Substituting (2.9) into (2.2) and (2.4) and making use of (2.2) and (2.7) we obtain

$$f'''+ff''-f'^2-A\left(f'+\frac{1}{2}\eta f''\right)+\lambda\theta=0, \tag{2.10}$$

$$\left((1+\varepsilon\theta+Nr)\,\theta'\right)' - \Pr\begin{vmatrix} f' & \theta' \\ f & \theta \end{vmatrix} - A\Pr\left(2\theta+\frac{1}{2}\eta\theta'\right) = 0, \tag{2.11}$$

$$\begin{aligned} &f'(\eta)=1, \quad f(\eta)=f_w, \quad \theta(\eta)=1 \quad \text{at } \eta=0,\\ &f'(\eta)\to 0 \quad \theta(\eta)\to 0 \quad \text{as } \eta\to\infty, \end{aligned} \tag{2.12}$$

where a prime denotes differentiation with respect to η, $|*|$ is the determinant, $A = C/a$ is the that unsteady parameter, $Nr = \frac{16\sigma^* T_\infty^3}{3K_\infty K^*}$ is the thermal radiation parameter, $\Pr = \frac{\nu}{\alpha_\infty}$ is the Prandtl number, $\alpha_\infty = \frac{K_\infty}{\rho C_p}$, $f_w = -\frac{v_w}{\sqrt{\nu a}}$. From the definition f_w it follows that the suction or injection parameter is used to control the strength and direction of the normal flow at the boundary. Further, λ is a dimensionless constant known as the buoyancy or free convection parameter defined as $\lambda = g\beta b/a^2$ where $\lambda > 0$ and $\lambda < 0$ correspond to assisting and opposing flows, respectively; while $\lambda = 0$ is for the forced convection flow situation. We noticed that in the absence of the unsteady parameter, variable thermal conductivity parameter, and impermeability of the boundary wall, Eqs. (2.10) and (2.11) reduce to those of Vajravelu [8], while in the absence of the free convection parameter the equations reduce to those of Grubka and Bobba [6]. Further when the thermal radiation and thermal conductivity parameter are absent the equations reduce to those of Ishak et al. [24]. Furthermore, when an unsteady parameter is zero and free convection parameter is zero, Eq. (2.11) has the closed form solution

$$f(\eta) = 1 - e^{-\eta} + f_w$$

while the solution for the energy equation (2.12) in terms of Kummer's functions is given by

$$\theta(\eta) = e^{-B_{21}\eta}\frac{M(B_{21}-2,\,1+B_{21};\,-\Pr e^{-\eta})}{M(B_{21}-2,\,1+B_{21};\,-\Pr)}, \qquad B_{21} = \Pr(1-f_w),$$

where $M(a, b, z)$ denotes the confluent hypergeometric function and is defined as follows

$$M(a,b,z) = 1 + \sum_{n=1}^{\infty}\frac{(a)_n z^n}{(b)_n n!}.$$

From the engineering point of view, the important characteristics of the flow are the skin-friction coefficient and the Nusselt number, respectively defined as

$$C_f = \frac{\tau_w}{\rho U_w^2/2}, \qquad \mathrm{Nu}_x = \frac{x q_w}{K_\infty (T_w - T_\infty)},$$

where the skin friction τ_ω and the heat transfer q_w from the sheet are given by

$$\tau_w = \mu\left(\frac{\partial u}{\partial y}\right)_{y=0}; \qquad q_w = -K_\infty\left(\frac{\partial T}{\partial y}\right)_{y=0}.$$

3. Numerical procedure

The boundary value problem (2.10)–(2.12) is solved by a second order finite difference scheme known as the Keller-box method [36,37]. The numerical solutions are obtained in four steps as follows:

- Reduce the equations to a system of first order equations;
- write the difference equations using central differences;
- linearize the algebraic equations by Newton's method, and write them in matrix–vector form; and
- solve the linear system by the block tri-diagonal elimination technique.

The step size $\Delta\eta$ and the position of the edge of the boundary layer η_∞ are to be adjusted for different values of the parameters to maintain accuracy. For numerical calculations, a uniform step size of $\Delta\eta = 0.01$ is found to be satisfactory and the solutions are obtained with an error tolerance of 10^{-6} in all the cases. For brevity, the details of the solution procedure are not presented here.

4. Results and discussion

By the Keller-box method the numerical results are obtained for several sets of values of the pertinent parameters, namely, the free convection parameter λ, the unsteady parameter A, the variable thermal conductivity parameter ε, the Prandtl number Pr and the thermal radiation parameter Nr for three cases (i) suction, (ii) injection and (iii) impermeable stretching sheet. To assess the accuracy of the computed results, numerical values for the wall temperature gradient are compared with the available results in the literature for the steady case ($A = 0$) and the resulted presented in Table 1: The results are found to be in good agreement. Also, to assess the effects of the various parameters on the flow and heat transfer characteristics, the numerical results are presented in Figs. 2–7 and in Table 2.

Table 1
Comparison of some of the values of wall temperature gradient $-\theta'(0)$ obtained by Grubka and Bobba [6], Ali [7] and Ishak et al. [24] with the present results in the absence of thermal radiation when $f_w = 0$.

A	λ	Pr	Grubka and Bobba [6]	Ali [7]	Ishak et al. [24]	Present results
0.0	0.0	0.01	0.0197	–	0.0197	0.019723
		0.72	0.8086	0.8058	0.8086	0.808836
		1.0	1.0000	0.9961	1.00000	1.000000
		3.0	1.9237	1.9144	1.9237	1.923687
		10.0	3.7207	3.7006	3.7207	3.720788
		10.0	12.2940	–	12.2941	12.30039
1.0	0.0	1.0	–	–	1.6820	1.681921
	1.0		–	–	1.7039	1.703910
0.0	1.0	1.0	–	–	1.0873	1.087206
	2.0		–	–	1.1423	1.142298
	3.0		–	–	1.1853	1.185197

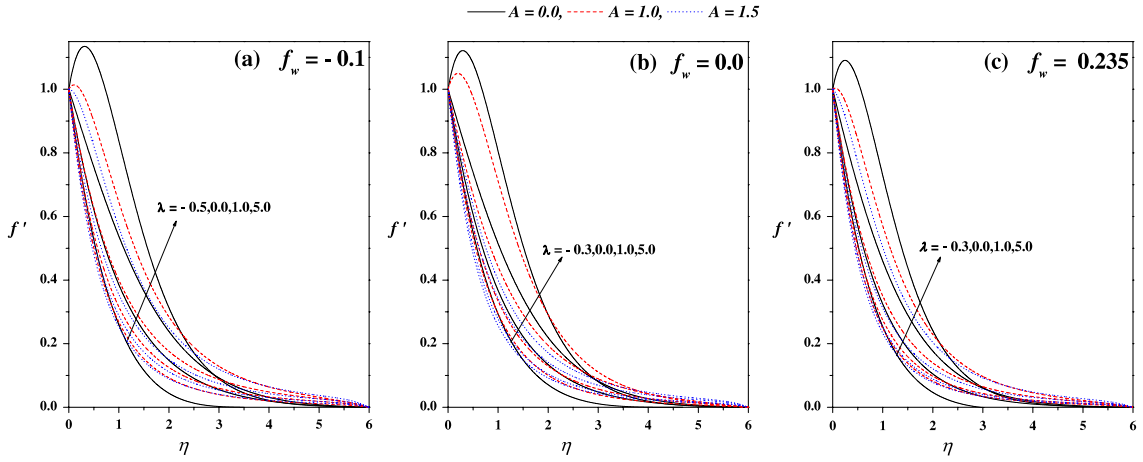

Fig. 2. Horizontal velocity profiles f' vs. η for different values of A and λ with $\varepsilon = 0.1$, $Nr = 0.1$.

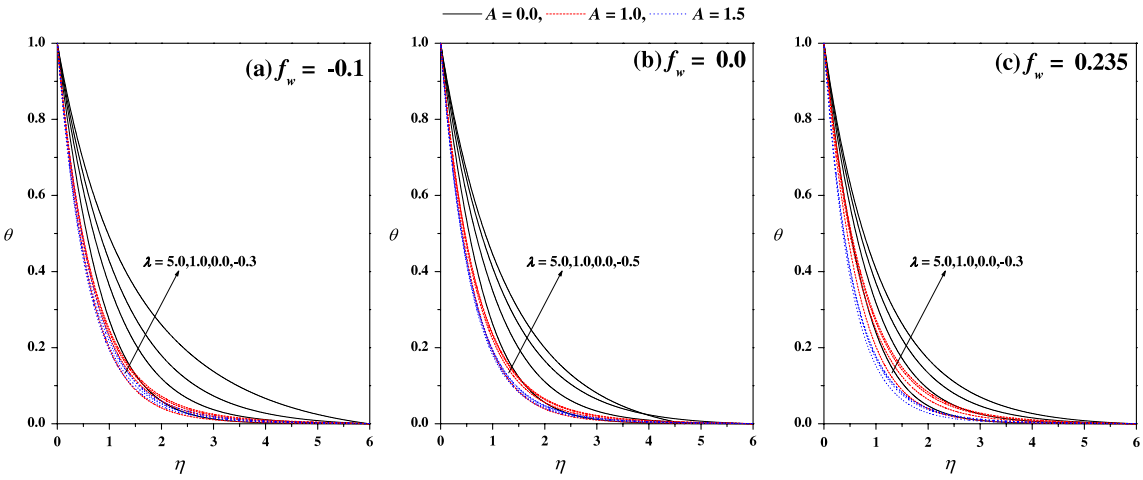

Fig. 3. Temperature profiles θ vs. η for different values of A and λ with $\varepsilon = 0.1$, $Nr = 0.1$.

Fig. 2(a)–(c) respectively show the effects of suction ($f_w < 0$), impermeability ($f_w = 0$) and the injection ($f_w > 0$) on the velocity field $f'(\eta)$ for different values of the free convection parameter λ and the unsteady parameter A with $\mathrm{Pr} = 1.0$ and $Nr = 0.1$ when $\varepsilon = 0.1$. From these figures it can be seen that the velocity profiles decrease monotonically to zero as the distance η increases from the boundary. However, in the case of steady flow ($A = 0$), the velocity profile increases from its value of one in the boundary layer and then decays to zero. The effect of increasing values of the free convection parameter λ is to increase the velocity $f'(\eta)$. Physically $\lambda > 0$ means heating of the fluid or cooling of the surface (assisting flow), $\lambda < 0$ means cooling of the fluid or heating of the surface (opposing flow) and $\lambda = 0$ means the absence of free

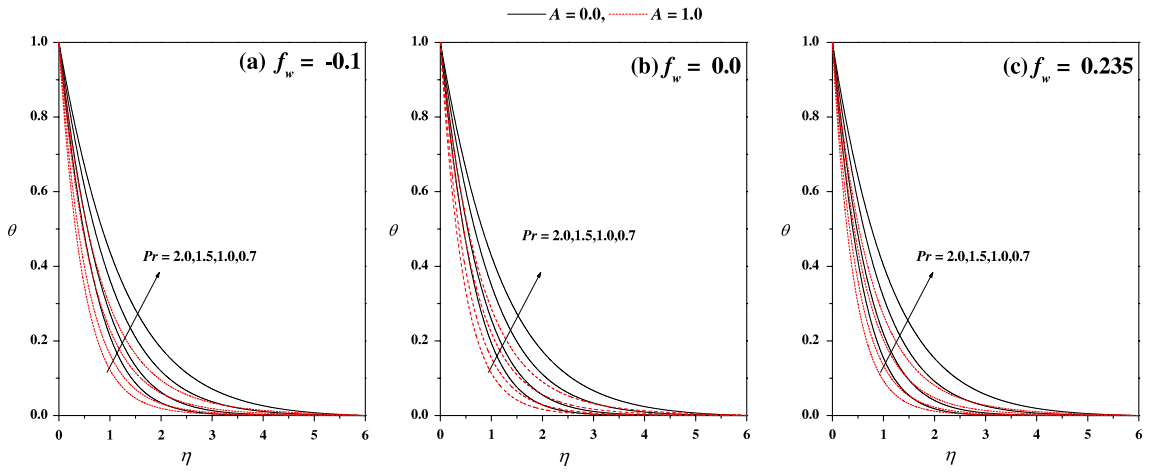

Fig. 4. Temperature profiles θ vs. η for different values of Pr and A with $\lambda = 1.0$, $\varepsilon = 0.1$, $Nr = 0.1$.

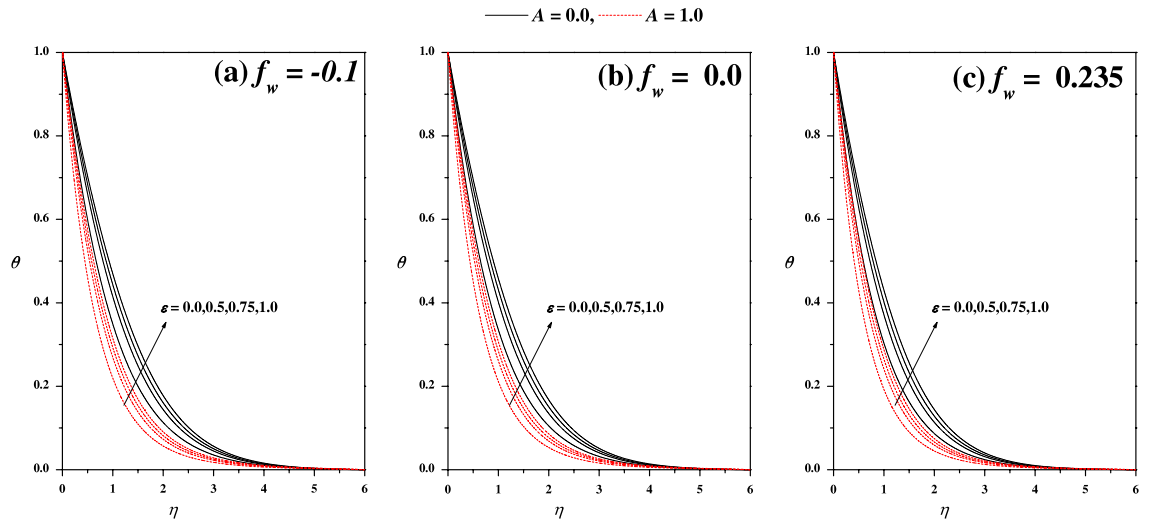

Fig. 5. Temperature profiles θ vs. η for different values of ε and A with $\lambda = 1.0$, Pr $= 1.0$, $Nr = 0.1$.

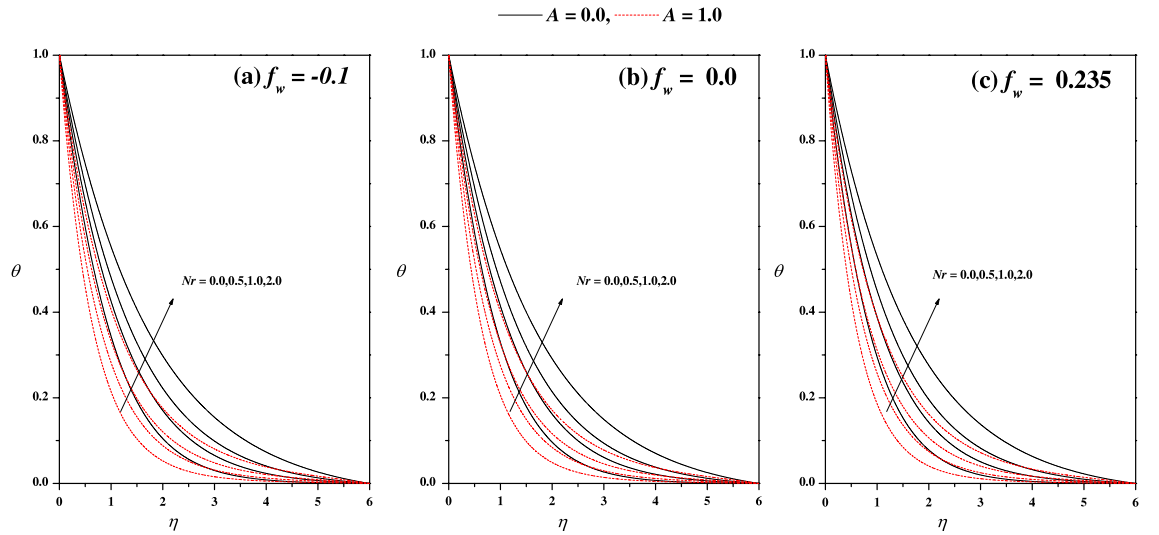

Fig. 6. Temperature profiles θ vs. η for different values of Nr and A with $\lambda = 1.0$, Pr $= 1.0$, $\varepsilon = 0.1$.

Table 2
Skin friction and wall temperature gradient for different values of pertinent parameters.

λ	ϵ	Nr	Pr	A	$f_w = -0.1$		$f_w = 0.0$		$f_w = 0.2$	
					$f''(0)$	$\theta'(0)$	$f''(0)$	$\theta'(0)$	$f''(0)$	$\theta'(0)$
			0.7		−0.445419	−0.776308	−0.486030	−0.801981	−0.593040	−0.865597
			1.0	0.0	−0.493067	−0.933987	−0.538258	−0.972561	−0.656808	−1.069239
			1.5		−0.547444	−1.151605	−0.597645	−1.212410	−0.728207	−1.366903
		0.1	2.0		−0.584649	−1.334393	−0.638053	−1.417815	−0.775284	−1.631904
			0.7		−0.911017	−1.244895	−0.951753	−1.271239	−1.055438	−1.335453
			1.0	1.0	−0.942237	−1.491270	−0.985163	−1.529710	−1.094341	−1.624162
			1.5		−0.977554	−1.828623	−1.022904	−1.887411	−1.138021	−2.033397
	0.1		2.0		−1.002073	−2.11066	−1.049023	−2.190301	−1.168025	−2.388745
		0.0			−0.505108	−0.975890	−0.551459	−1.018446	−0.672862	−1.125430
		0.5	1.0	0.0	−0.453826	−0.807167	−0.495188	−0.834975	−0.604099	−0.903996
		1.0			−0.418234	−0.702800	−0.456107	−0.723154	−0.556022	−0.773255
1.0		2.0			−0.371176	−0.576905	−0.404490	−0.589883	−0.492477	−0.621502
		0.0			−0.949962	−1.556255	−0.993436	−1.598351	−1.103979	−1.702018
		0.5	1.0	1.0	−0.916809	−1.293598	−0.957920	−1.322007	−1.062544	−1.391332
		1.0			−0.893122	−1.129368	−0.932539	−1.150655	−1.032852	−1.202305
		2.0			−0.860266	−0.928273	−0.897329	−0.942294	−0.991593	−0.976083
	0.0				−0.501637	−0.989538	−0.547387	−1.032214	−0.667241	−1.139260
	0.5				−0.463050	−0.775309	−0.506138	−0.802835	−0.619677	−0.871580
	0.75	0.1	1.0	0.0	−0.447030	−0.707614	−0.488913	−0.730782	−0.599519	−0.788518
	1.0				−0.432644	−0.654219	−0.473401	−0.674128	−0.581230	−0.723636
	0.0				−0.948746	−1.579272	−0.991983	−1.621739	−1.101892	−1.726154
	0.5				−0.919572	−1.240191	−0.961320	−1.267812	−1.067690	−1.335492
	0.75	0.1	1.0	1.0	−0.907577	−1.133173	−0.948647	−1.156536	−1.053373	−1.213690
	1.0				−0.896875	−1.048775	−0.937311	−1.068957	−1.040483	−1.118249
−0.3					−1.124402	−0.795733	−1.173691	−0.836590	−1.303475	−0.931273
0.0					−0.951792	−0.844385	−1.000489	−0.883698	−1.124728	−0.983985
0.5					−0.709921	−0.897441	−0.756747	−0.936146	−0.838252	−1.033746
1.0	0.1	0.1	1.0	0.0	−0.493067	−0.933987	−0.538258	−0.972561	−0.656808	−1.069239
2.0					−0.096665	−0.988166	−0.139165	−1.026678	−0.252503	−1.122539
5.0					0.947089	−1.094531	0.910504	−1.133060	0.809199	−1.228088
−0.3					−1.244570	−1.189590	−1.291938	−1.228022	−1.411025	−1.323824
0.0					−1.120973	−1.203367	−1.167325	−1.241820	−1.284701	−1.337440
0.5					−0.924787	−1.223508	−0.969649	−1.261989	−1.04381	−1.357399
1.0	0.1	0.1	1.0	0.5	−0.737664	−1.241201	−0.781214	−1.279706	−0.893522	−1.374967
2.0					−0.382776	−1.271753	−0.424048	−1.310295	−0.532008	−1.405350
5.0					0.586351	−1.342226	0.550423	−1.380835	0.453073	−1.475550
−0.3					−1.378658	−1.462216	−1.424645	−1.500553	−1.539654	−1.595035
0.0					−1.275302	−1.469366	−1.320522	−1.507732	−1.434085	−1.602208
0.5					−1.106744	−1.480654	−1.150773	−1.519061	−1.262070	−1.613525
1.0	0.1	0.1	1.0	1.0	−0.942237	−1.491270	−0.985163	−1.529710	−1.094341	−1.624162
2.0					−0.623398	−1.510869	−0.664323	−1.549363	−0.769610	−1.643787
5.0					0.273196	−1.560619	0.237224	−1.599213	0.141779	−1.693554
−0.3					−1.506090	−1.688248	−1.551316	−1.726552	−1.663851	−1.820368
0.0					−1.415048	−1.692853	−1.459660	−1.731177	−1.570987	−1.825007
0.5					−1.265177	−1.700303	−1.308807	−1.738658	−1.418198	−1.832507
1.0	0.1	0.1	1.0	1.5	−1.117469	−1.707495	−1.160164	−1.745878	−1.267703	−1.839743
2.0					−0.827889	−1.721194	−0.868834	−1.759625	−0.972890	−1.853515
5.0					0.002684	−1.757974	−0.003371	−1.796509	−0.128618	−1.890435

convection currents (forced convection flow). Also, an increase in the value of λ can lead to an increase in the temperature difference $(T_w - T_\infty)$: This leads to an enhancement of the velocity $f'(\eta)$ due to the enhanced convection currents and thus an increase in the boundary layer thickness. This is true even for different values of the unsteady parameter A. The effect of increasing values of the unsteady parameter A is to decrease the velocity $f'(\eta)$. This is true even with the suction parameter f_w. From Fig. 2(a)–(c), it can be seen that the suction reduces the velocity boundary layer thickness whereas the injection has the opposite effect. These results are consistent with the physical situation (see Table 2).

The temperature field $\theta(\eta)$ is shown graphically in Fig. 3(a)–(c) for different values f_w, the free convection parameter λ and the unsteady parameter A. An increase in the value of free convection parameter λ results in a decrease in the thermal boundary layer thickness and this results in an increase in the magnitude of the wall temperature gradient (see Table 2). This in turn produces an increase in the surface heat transfer rate. From Fig. 3(a) it can be noticed that the effect of increasing values of the unsteady parameter A is to decrease the temperature field and hence reduce the thermal boundary layer thickness. In general it is noticed that the effect of the unsteady parameter A on the temperature field is more noticeable

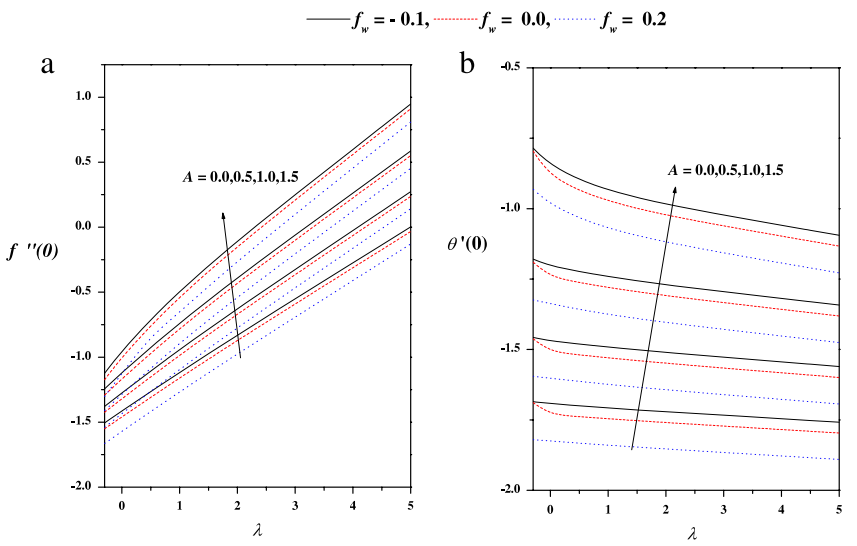

Fig. 7. (a) Skin friction $f''(0)$ vs. λ for different values of A and f_w with $\varepsilon = 0.1$, $Nr = 0.1$. (b) Wall temperature gradient $\theta'(0)$ vs. λ for different values of A and f_w with $\varepsilon = 0.1$, $Nr = 0.1$.

than on the velocity field. From Fig. 3 we see that the thermal boundary layer is thicker in the case of suction as compared to the case of impermeability: However, thinner in the case of blowing.

The variations of $\theta(\eta)$ for different values of the Prandtl number Pr and the unsteady parameter A are displayed in Fig. 4(a)–(c) with changes in f_w. The effect of increasing values of the Prandtl number Pr is to decrease the temperature $\theta(\eta)$. That is, an increase in Prandtl number Pr means a decrease in the thermal conductivity k_∞ and hence decreases of thermal boundary layer thickness. This can even be noticeable for zero and non-zero values of the unsteady parameter A. The effect of the variable thermal conductivity parameter ε on the temperature field (in the presence/absence of unsteady parameter A for the suction, impermeability and blowing upon the boundary wall cases) are depicted in Fig. 5(a)–(c). From these figures we can analyze that the temperature distribution is lower throughout the boundary layer in the absence of the variable thermal conductivity parameter ε and increases with the increasing values of the variable thermal conductivity parameter ε. This is due to the fact that the assumption of temperature dependent thermal conductivity implies reduction in the magnitude of the transverse velocity by a quantity $\frac{\partial}{\partial y}(k(T))$ which can be seen from the energy equation. This is even true for all values of f_w and the unsteady parameter A. The effects of thermal radiation parameter Nr on the temperature distribution $\theta(\eta)$ are shown in Fig. 6(a)–(c) for the zero and non-zero values of the unsteady parameter A. The effect of increasing values of the thermal radiation parameter Nr is to increase the temperature distribution in the flow region. From the graphical representation, it is observed that an increase in thermal radiation parameter Nr produces a significant increase in the thickness of the thermal boundary layer of the fluid. This is true even in the presence of the unsteady parameter A.

Numerical results for the skin friction $f''(0)$ and the Nusselt number $\theta'(0)$ with variations in λ and A for different values of f_w are shown in Fig. 7 respectively. It is seen from Fig. 7(a) that an assisting buoyant flow produces an increase in the skin friction, while an opposing buoyant flow produces the opposite effect. This is because the fluid velocity increases when the buoyancy force increases and hence increases the wall shear stress. This in turn increases the skin friction coefficient and as a consequence increases the heat transfer rate at the surface (see Fig. 7(b)). The impact of all the physical parameters on the skin friction $[-f_{\eta\eta}(0)]$ and the wall temperature gradient $[-\theta_\eta(0)]$ may be analyzed from Table 2. From Table 2 it can be seen that (as in Fig. 7(a)) the effect of the free convection parameter λ is to increase the skin friction and decrease the wall temperature gradient. The effect of the Prandtl number Pr is to decrease the wall temperature gradient; while the thermal radiation Nr and the variable thermal conductivity ε is to increase it. This phenomenon is even true in the presence of the unsteady parameter A.

5. Conclusion

Some of the interesting conclusions are as follows:

(i) It is observed that an increase in the unsteady parameter A is to decrease the thicknesses of the velocity and the thermal boundary layers.
(ii) This behavior is true in the presence of free convection currents λ. Furthermore, the Nusselt number increases with increasing Nr and ε, whereas the opposite is true with increasing A and Pr.
(iii) The thermal boundary layer is thicker in the case of suction as compared to the case of impermeability.
(iv) It is observed that an increase in thermal radiation parameter Nr produces a significant increase in the thickness of the thermal boundary layer of the fluid.

Acknowledgment

The authors appreciate the constructive comments of a reviewer which led to definite improvement in the paper.

References

[1] B.C. Sakiadis, Boundary layer behavior on continuous solid surfaces, AIChE J. 7 (1961) 26–28.
[2] L.E. Erickson, L.T. Fan, V.G. Fox, Heat and mass transfer on a continuous flat plate with suction/injection, Ind. Eng. Chem. Fundam. 5 (1966) 19–25.
[3] F.K. Tsou, E.M. Sparrow, R.J. Goldstein, Flow and heat transfer in the boundary layer on a continuous moving surface, Int. J. Heat Mass Transfer 10 (1967) 219–235.
[4] L.J. Crane, Flow past a stretching plate, Z. Angew. Math. Phys. 21 (1970) 645–647.
[5] P.S. Gupta, A.S. Gupta, Heat and mass transfer on a stretching sheet with suction or blowing, Can. J. Chem. Eng. 55 (1977) 744–746.
[6] L.G. Grubka, K.M. Bobba, Heat transfer characteristics of a continuous stretching surface with variable temperature, J. Heat Transfer — Trans. ASME 107 (1985) 248–250.
[7] M.E. Ali, Heat transfer characteristics of a continuous stretching surface, Heat Mass Transfer 29 (1994) 227–234.
[8] K. Vajravelu, Flow and heat transfer in a saturated porous medium over a stretching surface, Z. Angew. Math. Mech. 74 (1994) 605–614.
[9] V. Kolár, Similarity solution of axisymmetric non-Newtonian wall jets with swirl, Nonlinear Anal. RWA 12 (2011) 3413–3420.
[10] Y. Qin, T. Wang, G. Hu, The Cauchy problem for a 1D compressible viscous micropolar fluid model: analysis of the stabilization and the regularity, Nonlinear Anal. RWA 13 (2012) 1010–1029.
[11] M. Chen, Blowup criterion for viscous, compressible micropolar fluids with vacuum, Nonlinear Anal. RWA 13 (2012) 850–859.
[12] K. Vajravelu, Convection heat transfer at a stretching sheet with suction or blowing, J. Math. Anal. Appl. 188 (1994) 1002–1011.
[13] T.S. Chen, F.A. Strobel, Buoyancy effects in boundary layer adjacent to a continuous moving horizontal flat plate, J. Heat Transfer — Trans. ASME 102 (1980) 170–172.
[14] A. Moutsoglou, T.S. Chen, Buoyancy effects in boundary layers on inclined continuous moving sheets, J. Heat Transfer — Trans. ASME 102 (1980) 371–373.
[15] C.H. Chen, Laminar mixed convection adjacent to vertical continuously stretching sheets, Heat Mass Transfer 33 (1998) 471–476.
[16] A.A. Afifty, E.M. Aboeldahab, E.S. Mohammed, Similarity analysis in magneto hydrodynamics: Hall effects on forced convective heat and mass transfer on non-Newtonian power law fluid past a semi infinite vertical flat plate, Acta Mech. 177 (2005) 71–87.
[17] C.H. Chen, Forced convection over a continuous sheet with suction or injection moving in a flowing fluid, Acta Mech. 138 (1999) 1–11.
[18] M. Ali, F. Al-Youself, Laminar mixed convection from a continuously moving vertical surface with suction/injection, Heat Mass Transfer 33 (1998) 301–306.
[19] M.A.A. Hamad, I. Pop, M.A.I. Ismail, Magnetic field effects on free convection flow of a nanofluid past a vertical semi-infinite flat plate, Nonlinear Anal. RWA 12 (2011) 1338–1346.
[20] S. Sarkar, S. Ganguly, G. Biswas, Mixed convective heat transfer of nanofluids past a circular cylinder in cross flow in unsteady regime, Int. J. Heat Mass Transfer 55 (2012) 4783–4799.
[21] E.M.A. Elbashbeshy, M.A.A. Bazid, Heat transfer over an unsteady stretching surface with internal heat generation, Appl. Math. Comput. 138 (2003) 239–245.
[22] M. Abd El-Aziz, Radiation effect on the flow and heat transfer over an unsteady stretching sheet, Int. Commun. Heat Mass Transfer 36 (2009) 521–524.
[23] S. Mukhopadhyay, Unsteady boundary layer flow and heat transfer past a porous stretching sheet in the presence of variable viscosity and thermal diffusivity, Int. J. Heat Mass Transfer 52 (2009) 5213–5217.
[24] A. Ishak, R. Nazar, I. Pop, Boundary layer flow and heat transfer over an unsteady stretching vertical surface, Meccanica 44 (2009) 369–375.
[25] N. Kousar, S. Liao, Unsteady non-similarity boundary-layer flows caused by an impulsively stretching flat sheet, Nonlinear Anal. RWA 12 (2011) 333–342.
[26] A.M. Rohni, S. Ahmad, I. Pop, J.H. Merkin, Unsteady mixed convection boundary-layer flow with suction and temperature slip effects near the stagnation point on a vertical permeable surface embedded in a porous medium, Transp. Porous Media 92 (2012) 1–14.
[27] T.C. Chiam, Heat transfer with variable thermal conductivity in a stagnation point flow towards a stretching sheet, Int. Commun. Heat Mass Transfer 23 (1996) 239–248.
[28] M. Subhas Abel, N. Mahesha, Heat transfer in MHD viscoelastic fluid flow over a stretching sheet with variable thermal conductivity, non-uniform heat source and radiation, Appl. Math. Model. 32 (2008) 1965–1983.
[29] M. Subhas Abel, P.G. Siddheshwar, N. Mahesha, Effects of thermal buoyancy and variable thermal conductivity on the MHD flow and heat transfer in a power-law fluid past a vertical stretching sheet in the presence of a non-uniform heat source, Internat. J. Non-Linear Mech. 44 (2009) 1–12.
[30] M. Subhas Abel, P.S. Datti, N. Mahesha, Flow and heat transfer in a power-law fluid over a stretching sheet with variable thermal conductivity and non-uniform heat source, Int. J. Heat Mass Transfer 52 (2009) 2902–2913.
[31] A.T.M.M. Rahman, M.S. Alam, M.K. Chowdhury, Thermophoresis particle deposition on unsteady two-dimensional forced convective heat and mass transfer flow along a wedge with variable viscosity and variable Prandtl number, Int. Commun. Heat Mass Transfer 39 (2012) 541–550.
[32] A. Raptis, C. Perdikis, Viscoelastic flow by the presence of radiation, Z. Angew. Math. Mech. 78 (1991) 277–279.
[33] C. Perdikis, A. Raptis, Heat transfer of a micro polar fluid by the presence of radiation, Heat Mass Transfer 31 (1996) 381–382.
[34] A. Raptis, Radiation and visco elastic flow, Int. Commun. Heat Mass Transfer 26 (1999) 889–895.
[35] M.Q. Brewster, Thermal Radiative Transfer Properties, John Wiley and Sons, 1972.
[36] T. Cebeci, P. Bradshaw, Physical and Computational Aspects of Convective Heat Transfer, Springer-Verlag, New York, 1984.
[37] H.B. Keller, Numerical Methods for Two-Point Boundary Value Problems, Dover Publ., New York, 1992.